



## Simultaneous measurement of NO and NO<sub>2</sub> by dual-channel cavity ring down spectroscopy technique

Renzhi Hu (1)†\*, Zhiyan Li (1, 2) †, Pinhua Xie (1, 3, 5) \*, Hao Chen (1), Xiaoyan Liu(4),  
Shuaixi Liang (1, 2), Dan Wang (6), Fengyang Wang(1), Yihui Wang(1,3), Chuan Lin (1), Jianguo  
5 Liu(1, 3, 5), Wenqing Liu(1, 3, 5)

(1) Key Lab. of Environmental Optics and Technology, Anhui Institute of Optics and Fine Mechanics,  
Chinese Academy of Sciences, Hefei 230031, China.

(2) Science Island Branch of Graduate School, University of Science and Technology of China. Hefei  
230026, China.

10 (3) School of Environmental Science and Optoelectronic Technology, University of Science and  
Technology of China, Hefei 230027, China

(4) College of Pharmacy, Anhui Medical University, 81 Meishan Road, Hefei 230032, China

(5) CAS Center for Excellence in Regional Atmospheric Environment, Institute of Urban Environment,  
Chinese Academy of Sciences, Xiamen, 361000, Fujian, China

15 (6) School of Mathematics and Physics, Anhui University of Technology, Ma an Shan 243032, China

†These authors contributed equally to this work.

\*e-mail: rzhu@aiofm.ac.cn, phxie@aiofm.ac.cn

Key words: NO<sub>x</sub>; CRDS; CEAS; CL

### 20 Abstract

Nitric oxide (NO) and nitrogen dioxide (NO<sub>2</sub>) are relevant to air quality due to their role in  
tropospheric ozone (O<sub>3</sub>) production. In China, NO<sub>x</sub> emissions are high and exhausted from on-road  
vehicles make up 20% of total NO<sub>x</sub> emissions. Too much NO<sub>x</sub> are harmful to the human body and  
animals. In order to detect the NO and NO<sub>2</sub> emissions on road, a dual-channel CRDS system for NO<sub>2</sub>  
25 and NO detection is reported. In this system, NO is converted to NO<sub>2</sub> by its reaction with excess O<sub>3</sub> in  
NO<sub>x</sub> channel, such that NO can be determined through the difference between two channels. The  
detection limits of the developed CRDS system for NO<sub>2</sub> and NO<sub>x</sub> measurements are estimated to be  
about 0.030 ppb (1σ, 1 s) and 0.040 ppb (1σ, 1 s), respectively. Considering the error sources of NO<sub>2</sub>  
absorption cross section and R<sub>L</sub> determination, the total uncertainty of NO<sub>2</sub> measurements is about 5%.  
30 The CRDS method is capable of measuring species with high sensitivity and accuracy. The  
performance of the system was validated against a chemiluminescence (CL) analyzer (42i, Thermo  
Scientific, Inc.) when measuring the NO<sub>2</sub> standard mixtures. The results of NO<sub>2</sub> with standard mixtures  
sampled showed a linear correction factor (R<sup>2</sup>) of 0.99 in a slope of 1.031 ± 0.006, with an offset of  
(-0.940 ± 0.323) ppb. An intercomparison between the system and a cavity-enhanced absorption  
35 spectroscopy (CEAS) instrument for NO<sub>2</sub> measurement was also conducted alone in ambient  
environment. Least-squares analysis showed that the slope and intercept of the regression line are 1.042  
± 0.002 and (-0.393 ± 0.040) ppb, respectively, with a linear correlation factor of R<sup>2</sup> = 0.99. Another  
intercomparison conducted between the system and the CL analyzer for NO detection also showed a  
good agreement within their uncertainties, with an absolute shift of (0.352 ± 0.013) ppb, a slope of  
40 0.957 ± 0.007 and a correlation coefficient of R<sup>2</sup> = 0.99. The measurements of on-road vehicle emission  
plumes by this mobile CRDS instrument show the different emission characteristics in the urban and



suburban areas of Hefei. The instrument provides a new method for retrieving fast variations of NO and NO<sub>2</sub> plumes.

## 1. Introduction

45 In recent years, with the improvement of people's living standard, people pay more and more  
attention to the improvement of the living environment. Among which, the management of  
environmental pollution has gradually become one of the focus issues. The detection of pollutants is an  
important premise for environmental governance. NO<sub>x</sub> (NO<sub>x</sub>= NO+NO<sub>2</sub>) are byproducts of organic  
50 power generation using fossil fuels) (Jaramillo and Muller, 2016) and mobile sources (motor vehicles  
and catalytic converters of most cars) (Carslaw, 2005). NO<sub>x</sub> are both primary pollutants and secondary  
pollutants (Crutzen, 1979), which can determine the tropospheric O<sub>3</sub> levels and lead to the formation of  
photochemical "smog" and the visibility decline due to the secondary aerosol formation. Furthermore,  
NO<sub>x</sub> are also the precursors of nitric acid (Brown et al., 2004). Moreover, NO<sub>x</sub> are harmful to the  
55 human body and animals. Too much high NO<sub>x</sub> can damage the respiratory system and lead to  
pulmonary edema (Yang and Omaye, 2009). In addition, accurate NO<sub>2</sub> measurement plays a key role in  
accurate measurement of other species, such as organic nitrate (Thieser et al., 2016; Paul et al., 2009;  
Day et al., 2002) and RO<sub>2</sub> radicals (Chen et al., 2016).

During the last few years, many direct and indirect techniques for monitoring NO<sub>2</sub> have been  
60 established. NO<sub>2</sub> concentration can be measured with chemiluminescence (CL) detection (Yuba et al.,  
2010; Sadanaga et al., 2008; Fahey et al., 1985), differential optical absorption spectroscopy (DOAS)  
(Platt et al., 1984; McLaren, 2010), tunable diode laser absorption spectroscopy (TDLAS) (Li et al.,  
2004), cavity ring-down spectroscopy (CRDS) (Castellanos et al., 2009; Fuchs et al., 2009; Osthoff et  
65 al., 2006; Fuchs et al., 2010; Brent et al., 2013 ; Hu et al., 2015), cavity enhanced absorption  
spectroscopy (CEAS) (Wu et al., 2009; Gherman et al., 2008; Kasyutich et al., 2006; Wada and  
Orr-Ewing, 2005), cavity attenuated phase shift spectroscopy (CAPS) (Kebabian et al., 2008),  
laser-induced fluorescence (LIF) (Taketani et al., 2007; Matsumi et al., 2010; Sadanaga et al., 2014;  
Matsumoto et al., 2001) measurement, long path absorption photometer (LOPAP) (Villena et al., 2011)  
70 and gas based sensors (Novikov et al., 2016), with CL being the most widely used for ambient in situ  
sampling. CL can achieve direct measurement of NO and indirect measurement of NO<sub>2</sub>. The method is  
based on the reaction between NO and O<sub>3</sub>, which can form an electronically excited molecule of NO<sub>2</sub>\*.  
When NO<sub>2</sub>\* reaches the ground state, it emits fluorescence which is proportional to the NO value. NO<sub>2</sub>  
is measured by its conversion to NO and usually heated (300 °C to 350 °C) molybdenum (Mo) surfaces  
(Ridley and Howlett, 1974) or photolytic NO<sub>2</sub> converters like Xenon lamps or UV emitting diodes at  
75 specific wavelength (320 nm-400 nm) are used. The CL instruments have typical NO<sub>2</sub> detection limits  
of 50 ppt / 1 min (1σ) (Wang et al., 2001). CRDS, CEAS, CAPS and TDLAS relying on scanning a  
light source through a range of frequencies of interest are all direct absorption techniques. These  
techniques can achieve a high sensitivity of several seconds and a low detection limit of ppt level (Li et  
al., 2004; Wild et al., 2014; Gherman et al., 2008; Kebabian et al., 2008). Among these techniques,  
80 CRDS has become a promising technique for ambient NO<sub>2</sub> detection due to its advantages of high time  
resolution, low detection limit as well as portability, in which pulsed (Fuchs et al., 2009) and  
continuous-wave (cw) (Wada and Orr-Ewing, 2005) lasers were utilized. Wada et al. (Wada and  
Orr-Ewing, 2005) demonstrated a cw diode CRDS system operating at 410 nm for the retrieval of NO<sub>2</sub>  
mixing ratios in ambient air with a detection limit of 0.1 ppb in 50 s at atmospheric pressure. Osthoff et



85 al. (Osthoff et al., 2006) constructed a pulsed cavity ring-down spectrometer which used a pulsed (20–  
100 Hz, up to 25 mJ) frequency-doubled Nd:YAG laser for the simultaneous measurements of NO<sub>2</sub>,  
nitrate radical (NO<sub>3</sub>), and dinitrogen pentoxide (N<sub>2</sub>O<sub>5</sub>) in the atmosphere. The NO<sub>2</sub> detection limit (1σ)  
for 1 s data was 40 ppt with an uncertainty within ±4% under laboratory conditions. Fuchs (Fuchs et  
90 al., 2009) used a simple, lightweight, low power, commercially available Fabry-Perot (FP) diode laser  
with a center wavelength of 403.96 nm as a light source to detect NO and NO<sub>2</sub> in two separate channels.  
The limit of detection is 22 ppt (2σ precision) for NO<sub>2</sub> at 1 s time resolution. Karpf (Karpf et al., 2016)  
used a high-power, multimode Fabry Perot (FP) diode laser with a broad wavelength range ( $\Delta\lambda_{\text{laser}} \sim$   
0.6 nm) to excite a large number of cavity modes, thereby reducing the susceptibility of the detector to  
vibration and making it well suited for field deployment. A sensitivity of 38 ppt was achieved using an  
95 integration time of 128 ms for single-shot detection. A number of intercomparison studies  
demonstrating the accuracy of these research grade instruments have been carried out (Xu et al., 2013;  
Dunlea et al., 2007; Villena et al., 2012) to evaluate the uncertainty of each instrument. The comparison  
results show that the method based on Mo converters is affected by significant interferences such as  
N<sub>2</sub>O<sub>5</sub>, HONO, HNO<sub>3</sub>, PAN, etc. Whereas the method based on optical absorption is relatively immune  
100 to interferences. Therefore, direct techniques are considered to be more reliable methods than the CL  
method for the measurement NO<sub>2</sub> and have also been used in field experiments (Ayres et al., 2015;  
Wagner et al., 2013; Sobanski et al., 2016).

In addition to the direct measurement of NO with the CL method, NO concentrations can be  
measured based on their absorption feature at 1,585.282 cm<sup>-1</sup> directly. For this method, a tunable  
105 infrared laser differential absorption spectroscopy (TILDAS) instrument, utilizing an astigmatic  
multi-pass Herriott cell (Herndon et al., 2004) and a dual-wavelength spectrometer, based on a DFB  
laser emitting sequentially at 1,600 cm<sup>-1</sup> and 1,900 cm<sup>-1</sup> have been used for the measurement of the two  
species (Jagerska et al., 2015). The 1 s precision for NO measurement of the TILDAS instrument was  
550 ppt, whereas that for the field experiments was 1.5 ppb. Thus, this technique may suffer from low  
110 detection sensitivity compared with the CL method. Given the rapid changes of nighttime oxidation,  
i.e., NO<sub>3</sub> radical, understanding the rapid changes of its precursors, NO and NO<sub>2</sub> is thus a critical  
prerequisite information to develop a nighttime atmospheric chemistry model. Conversion to NO<sub>2</sub> by  
adding excess O<sub>3</sub> can provide an indirect method for NO detection, which can achieve high sensitivity  
and high resolution (Fuchs et al., 2009; Wild et al., 2014).

115 The development of different technology provide the potential for NO<sub>x</sub> measurements on  
different platforms such as ground sites, vehicles as well as aircrafts (Yamamoto et al., 2011; Wagner  
et al., 2011; Castellanos et al., 2009). Due to the rapid economic growth in 2000-2010, China has become  
the second largest economy in the world. With the rapid growth of energy consumption, NO<sub>x</sub> emissions  
is increasing. Motor vehicles are one of the major sources for NO<sub>x</sub>, especially in urban areas  
120 (Westerdahl, 2008). Exhaust from on-road vehicles makes up 20% of total NO<sub>x</sub> emissions in China  
(Shi et al., 2014). So a variety of methods have been used to measure the vehicle emissions to access  
air pollutant exposures and specifically impacts due to traffic-related emissions (Vogt et al., 2003;  
Carslaw and Beevers, 2004; Herndon et al., 2005; Lal et al., 2005; Burgard et al., 2006b; Hueglin et al.,  
2006; Burgard et al., 2006a; Wild et al., 2017). However, the methods are usually applied to monitor air  
125 pollutants at several locations in large cities, the selection of which is critical for achieving  
representative measurements. The number of monitoring locations is not adequate to show the large  
scale patterns of the city. Hence, a direct on-road mobile instrument can be used to help obtain the  
spatial and temporal variations of NO<sub>x</sub> pollutants.



Here, we describe a dual-channel CRDS system based on the chemical conversion NO to NO<sub>2</sub> to  
130 measure NO<sub>2</sub> and NO<sub>x</sub> simultaneously. In one channel, the sum of converted NO<sub>2</sub> from ambient NO  
and ambient NO<sub>2</sub> is determined to provide a direct measurement of NO<sub>x</sub>. In another channel, only  
ambient NO<sub>2</sub> is measured. The subtraction of NO<sub>2</sub> measured in a second, independent channel provides  
a direct measurement of NO alone. Measurements and comparison of NO<sub>2</sub> and NO between different  
135 instruments were conducted to assess the accuracy of the dual-channel CRDS instrument. In addition,  
the measurement of on-road vehicle emission plumes from the instrument during December 17, 2018 in  
the region of Hefei, China was deployed. The main advantages of this instrument compared with CL  
instruments are its low detection limit and high sensitivity as well as its potential ability for trace  
measurements without calibration and interferences.

## 2. Setup of the instrument

140 Cavity ring-down spectroscopy has been applied to measurement NO<sub>3</sub> radical and N<sub>2</sub>O<sub>5</sub> in our  
group (Wang et al., 2015; Li et al., 2018; Li et al., 2018). In this work, the technique is applied to  
measure NO<sub>2</sub> and NO. A schematic diagram of the dual-channel CRDS system developed in the present  
work is shown in Fig. 1. The instrument mainly consists two identical CRDS systems for NO<sub>2</sub> and NO<sub>x</sub>  
detection, gas handling system, NO convertor and activated carbon device for NO<sub>x</sub> removing.

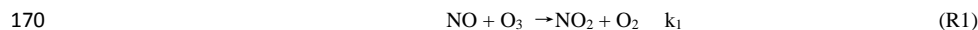
### 145 2.1. CRDS systems

A blue diode laser is used as the light source and the wavelength of the laser is monitored by a  
spectrometer. The output of the diode laser with a center wavelength at 403.64 nm and a line width of  
0.5 nm is directly modulated by a square wave signal (on/off) at a repetition of 2 kHz with a duty cycle  
of 50% and the output power is about 60 mW. The light emitted by the laser first passes through an  
150 isolator to prevent the reflected light into the laser and then enters into two identical cavities through  
two reflecting mirrors and a 50/50 beam splitter. Each optical cavity is made of an aluminum tube with  
an inner diameter of 9.4 cm. The two cavities are fixed rigidly by two frames, respectively. Two high  
reflectivity mirrors are held in stable, adjustable mounts. The distance of two highly reflective mirrors  
(LGR, 1 in. diameter, 1 m radius of curvature) is 75 cm for both channels. Consequently, ring-down  
155 time constants in NO<sub>x</sub> and NO<sub>2</sub> cavities are 22.90 μs and 24.12 μs in dry N<sub>2</sub>. The light emitted through  
the back mirror of the cavity passes through a narrowband filter to filter stray light and then is directed  
into a PMT. The signal passes through an amplifier and then enters into the digital acquisition card (NI  
USB-6361, 16-bit, 2.0 Ms/s). The digital acquisition card is 1 MHz for each channel. Data are acquired  
on the data acquisition board for a continuous period of 1.0 s during which 2000 decay traces are  
160 transferred to the PC using a single transfer command and averaged to get a fitted decay trace at a laser  
modulation rate of 2 KHz. The software algorithms calculate NO<sub>2</sub> concentration from,  $\tau$  and  $\tau_0$ , the  
ring-down time when the NO<sub>2</sub> is in the presence and absence of the cavity, respectively; the NO<sub>2</sub>  
absorption cross section,  $\sigma$ ; the ratio of the total cavity length to the length over which the absorber is  
present in the cavity,  $R_L$  and the speed of the light,  $c$ . The concentration of the sample can be expressed  
165 as follows:

$$[\text{NO}_2] = \frac{R_L}{c \sigma_{\text{NO}_2}} \left( \frac{1}{\tau} - \frac{1}{\tau_0} \right) \quad (1)$$

### 2.2. NO convertor

NO is measured by its conversion to NO<sub>2</sub> by adding excess O<sub>3</sub>. The principle is based on the  
following chemical equation (Sander et al., 2006).



Where  $k_1 = 3.0 \times 10^{-12} \exp(-1310/T) \text{ cm}^3 \text{ molec}^{-1} \text{ s}^{-1}$ . Ozone is produced from  $\text{O}_2$  photolysis at 185 nm by flowing 100 sccm of sampling air which is controlled by a MFC over a low pressure discharge mercury lamp. The mercury is inset into a quartz glass tube with a length of 50 mm and an inner diameter of 10mm. The flow rate passing through the mercury lamp was investigated and the resulting mixing ratio of  $\text{O}_3$  was detected by an  $\text{O}_3$  analyzer (49i, Thermo Scientific). The  $\text{O}_3$  concentration is approximately 11.2 ppm after mixing with the sampled air. A length of Teflon tubing (length 1 m, i.d. 3.8mm) serves as a reactor for the NO conversion.

175

### 2.3. Activated carbon device

Background measurement of  $\tau_0$ , that is the ring down time when the absorber is in the absence of the cavity, is important for accurately retrieving the absorber concentration as well as for checking the cleanliness of the cavity mirrors. Usually zero air or chemical scrubber is used to acquire zeros (Wada and Orr-Ewing, 2005). In our system, zeros are obtained by passing sampled air through an activated carbon filled tubing with an outer diameter of 6.0 cm and a length of 26.0 cm through a three-way solenoid valve located below the filter holder. The  $\tau_0$  is measured for 60 s every 10–16 min. This frequency of zero measurements is observed to be sufficient to track drifts in the zero ring-down time constant measurement, with a stability of successive  $\tau_0$  below 0.1% for 15 min intervals.

180

185

### 2.4. Gas handling system

The instrument gas handling system consists of sampling module and purge flow. The sampled air initially flows through a filter device loaded with filtering membrane (1  $\mu\text{m}$  pore size) to prevent light-scattering aerosols from entering the cavity with a rotary pump (K86KNE) and subsequently passes through the activated carbon device to provide the background measurement when the three-way solenoid valve is open or is directed toward the PFA tube when the three-way solenoid valve is closed. The air flow from the PFA tube is divided into three lines. Among which, 100 sccm sampled air, which is introduced into a quartz flow tube equipped with a mercury pen-ray lamp (Oriol 6035) to generate  $\text{O}_3$  by air photolysis as mentioned previously is merged with another 900 sccm sampled air and pulled into the  $\text{NO}_x$  cavity. The third flow with a flow rate of 1 slm is directed into the  $\text{NO}_2$  cavity. The flow rates of all of the gases are controlled by mass flow controllers. Each mirror is isolated from the sample flow by a purge volume that is continuously flushed with high-purity nitrogen at a rate of 25  $\text{ml min}^{-1}$  to prevent the degradation of the mirror reflectivity.

190

195

## 200 3. Results and discussion

### 3.1 Determination of Absorption Cross Sections

To retrieval the gas concentration, it is vital to determine the effective absorption cross section at peak absorption of the laser. The output waveforms of the laser, with a center wavelength of 403.64 nm and full width at half-maximum of 0.5 nm, was monitored by a spectrometer (QEPB0828) (red line shown in Fig. 2). The center wavelength selected can cover the strong absorption of  $\text{NO}_2$  and avoid the interference from other species, such as  $\text{H}_2\text{O}$  (pink line in Fig. 2). The effective absorption cross section was determined to be  $5.63 \times 10^{-19} \text{ cm}^2 / \text{molecule}$  by convolution the  $\text{NO}_2$  absorption cross section by voigt (Voigt et al., 2002) with the laser spectrum (blue line in Fig. 2). A shift in the laser center wavelength would result in a change of the effective  $\text{NO}_2$  cross-section. The day-to-day variability of

205



210 the laser center wavelength was less than 1% by monitoring the laser output for a few days. The largest  
uncertainty of the absorption cross section is about 3% according to Voigt (Voigt et al., 2002).

### 3.2 The retrieval of $R_L$

215 Due to the purge gas to the mirrors, the  $R_L$  value cannot be simply determined by the ratio of the  
distance between two mirrors to that between the inlet and outlet. The  $R_L$  value was determined from  
the absorption measurement of different concentrations of  $\text{NO}_2$  ranging from 20 ppb to 70 ppb in the  
presence and absence of purge flow. The ratio of the two extinction measurements yielded a  $R_L$  value  
independent of the  $\text{NO}_2$  cross section and concentration. The  $R_L$  value is determined to be  $1.10 \pm 0.03$   
for both the  $\text{NO}_x$  and  $\text{NO}_2$  channels.

### 3.3 The retrieval of $\tau_0$

220 In order to accurately determine the concentrations of trace gas by CRDS, it is very important to  
confirm background cavity loss measurements of  $\tau_0$  when the target gases are not inside the cavity.  
Several alternative background measurement methods which incorporate zero air, a mixture of oxygen  
and nitrogen, chemically scrubbed laboratory air (using hydroxyapatite), and laboratory air sampled  
through the stainless steel tubing coil have been reported (Wada and Orr-Ewing, 2005) and each  
225 experimental approach has its own merits and demerits. In our instrument, an activated carbon device  
was used for background measurement. The ring down times when the sampled air pass through the  
activated carbon device were determined to be  $24.12 \pm 0.01 \mu\text{s}$  and  $22.90 \pm 0.01 \mu\text{s}$  in two cavities,  
respectively. These values are close to those of measurements of zero air at the same sample rate for a 5  
min period.

230 Two representative ring-down signals of the  $\text{NO}_2$  from CRDS system when the  $\text{NO}_2$  is in the  
presence and absence of the cavity are shown in Fig. 3. And the fitted ring down time were  $24.12 \mu\text{s}$   
and  $20.30 \mu\text{s}$  respectively such that the  $\text{NO}_2$  concentration is 20.28 ppb using the constants determined  
above.

### 3.4 Detection limit and measurement accuracy of two cavities.

235 The measurement precision of the dual-channel CRDS instrument for  $\text{NO}_2$  and  $\text{NO}_x$  detection was  
investigated with time series measurement of zero air (Fig. 4). The acquisition time for the spectral data  
was 1.0 s with an average of 2000 spectra. In order to analyze the stability of the instrument, the Allan  
variance had been calculated for the intensity measurements. For the two channels, the minima in the  
Allan plots indicated the optimum average times for optimum detection performance (right panel of Fig.  
240 4) to be about 30 s. With 30 s integration time, the  $1\sigma$  detection limits were 16 ppt and 14 ppt for the  
 $\text{NO}_2$  and  $\text{NO}_x$  channels, respectively.

The minimum detection can be written as follows:

$$[A]_{\min} = \frac{\sqrt{2}R_L}{c\sigma} \left( \frac{\Delta\tau_0}{\tau_0} \right) \quad (2)$$

245 For continuous zero  $\text{NO}_2$  measurements, the  $\Delta\tau_0$  was  $0.008 \mu\text{s}$  in both  $\text{NO}_x$  and  $\text{NO}_2$  channels and  
 $\tau_0$  was  $22.90 \mu\text{s}$  and  $24.12 \mu\text{s}$  in  $\text{NO}_x$  and  $\text{NO}_2$  channels, respectively when averaging the data to 1 s.  
Taking the  $R_L$  value to be 1.10 and  $\sigma$  to be  $5.63 \times 10^{-19}$  molecule/cm<sup>2</sup>. The  $1\sigma$  minimum detection limits  
determined from the previously presented equation for the  $\text{NO}_x$  and  $\text{NO}_2$  channels are 39 ppt and 35 ppt  
at an integration time of 1 s, respectively, which were close to the Allan variance analysis described  
above.

250 The total uncertainty of  $\text{NO}_2$  measurement by CRDS was from the errors in  $R_L$  and the  $\text{NO}_2$



absorption cross section. The uncertainty in  $R_L$  was less than 3%, and the uncertainty in the  $\text{NO}_2$  absorption cross-section was about 4%. Considering all of these errors, the total uncertainty of  $\text{NO}_2$  measurement was determined to be 5%.

255 The minimum detection and uncertainty of our instrument is further compared with the existing field measurement techniques for  $\text{NO}_2$  measurements. (Table 1).

### 3.5 NO Conversion Efficiency

260 The main factor determining the NO conversion efficiency was the flow rate passing through the mercury pen-ray lamp which therefore influences the generated  $\text{O}_3$  concentration. The mixing ratio of  $\text{O}_3$  in the  $\text{NO}_x$  channel line changing with the flow rate that passes through the mercury pen-ray lamp was investigated and the result was shown in Fig. 5. As a result, the bypass flow passing through the Hg lamp was determined to be 100 sccm. Under this condition, when the residence time of  $\text{O}_3$  in the cavity is 1s and ambient  $\text{NO}_2$  concentration is 50 ppb, NO conversion efficiency with different NO concentrations (10-1000 ppb) is simulated and NO conversion efficiency is larger than 98% .

265 Because the cross section of  $\text{O}_3$  is about four orders magnitude of smaller than that of  $\text{NO}_2$  at the center wavelength of the laser, the absorption of  $\text{O}_3$  generated by mercury photolysis is negligible. According to Fuchs (Fuchs et al., 2009), under conditions when NO abundance is rich, further oxidation of  $\text{NO}_2$  to  $\text{NO}_3$  and  $\text{N}_2\text{O}_5$  has only a slight effect on  $\text{NO}_x$  measurement, such that correction of the  $\text{NO}_x$  measurement can be neglected. However, under conditions when NO is absent, the loss of  $\text{NO}_2$  due to oxidation by high concentration of ozone is indeed one of the main factors that attributes to  
270 the errors in the  $\text{NO}_x$  channel. The reaction equation is expressed as follows:



275 where  $k_2 = 1.2 \times 10^{-13} \exp(-2450/T) \text{ cm}^3 \text{ molec}^{-1} \text{ s}^{-1}$  ( $T=298\text{K}$ ,  $k_2 = 3.2 \times 10^{-17} \text{ cm}^3 \text{ molec}^{-1} \text{ s}^{-1}$ ) (Sander et al., 2006),  $k_{eq} = (5.1 \pm 0.8) \times 10^{-27} \exp(10871/T) \text{ cm}^3 \text{ molec}^{-1} \text{ s}^{-1}$  ( $T=298\text{K}$ ,  $k_{eq} = 3.5 \times 10^{-11} \text{ cm}^3 \text{ molec}^{-1} \text{ s}^{-1}$ ) (Osthoff et al., 2007) respectively. The loss rate will increase with the increase in the  $\text{NO}_2 + \text{O}_3$  reaction rate constant when temperature in the cavity increases. Moreover, the loss rate is sensitive to the  $\text{NO}_2$  mixing ratio. Diluted  $\text{NO}_2$  standard mixture was introduced into two channels to characterize the effect of high concentration ozone on  $\text{NO}_2$  measurement. The  $\text{NO}_2$  concentrations and the correlation plot between data in the two channels are shown in Fig. 6. The interference of  $\text{O}_3$  in  $\text{NO}_x$   
280 channel when NO is absent can be neglected. The discrepancy between two different channels may be caused by the systematic errors in two different channels and can be corrected with the coefficient obtained from Fig. 6 (b).

## 4. Field applications

### 4.1 Standard mixtures of NO and $\text{NO}_2$ measurement.

285 The comparisons of  $\text{NO}_2$  measurements between CRDS and  $\text{NO}_x$  analyzer have been carried out on  $\text{NO}_2$  standard mixtures. Different mixing ratios of  $\text{NO}_2$  were obtained by gas phase titration of NO with excess  $\text{O}_3$ , which was generated by an ozone generator (OC500). The 10.3 ppm NO standard mixture was initially diluted by  $\text{N}_2$  and subsequently oxidized by  $\text{O}_3$ . The amount of  $\text{NO}_2$  generated



from excess ozone can be calculated from the known initial concentration of NO. The generated pure  
290 NO<sub>2</sub> standards in clean air were in the concentration range of 20-70 ppb. The CL analyzer used for  
comparison in this laboratory experiment was separately calibrated and the linearity of this instrument  
was checked using a mixture containing NO. Fig. 7 (a) shows the concentration of standard NO<sub>2</sub> in the  
laboratory measured by CRDS and simultaneously by a commercial CL analyzer (42i, Thermo  
Scientific, Inc., 0.4 ppb (1 $\sigma$ ) detection limit). A correlation analysis between data from the two  
295 instruments was carried out. The fitting results shown in Fig. 7(b) indicate that NO<sub>2</sub>(CRDS) = NO<sub>2</sub>(CL  
analyzer)  $\times$  1.031 - 0.940, with a linear correlation factor (R<sup>2</sup>) of 0.99. The results in Fig. 7 (a) also  
indicates that CRDS instrument can capture the NO<sub>2</sub> variation more rapidly than CL analyzer.

#### 4.2 Ground-based measurements of NO<sub>2</sub> and NO.

The NO<sub>2</sub> concentration measured by the dual-channel CRDS instrument was compared with the  
300 results obtained by a CEAS instrument (Duan et al., 2018) during the period from November 3 to 5,  
2017 in the western suburb area of Hefei, Anhui, China. The CEAS instrument not the CL analyzer was  
selected for NO<sub>2</sub> intercomparison because the CL analyzer must convert NO<sub>2</sub> to NO, exposing itself to  
chemical interferences whereas the CEAS instrument directly detects NO<sub>2</sub>. Measurement precisions  
(1 $\sigma$ ) for NO<sub>2</sub> is about 170 ppt in 30 s. The time resolution of CRDS and CEAS instruments are 1s and  
305 1min respectively. The CRDS and the CEAS instruments were setup on the sixth floor of the building  
but apart by tens of meters in Anhui Institute optic and Fine mechanics. The area directly (1–1.5 km)  
to the northeast and the south of the site is the Dongpu reservoir. The area in the northwest to north sector  
is surrounded by a mix of trees. The significant NO<sub>2</sub> pollution directly found during the measurement is  
the emission of the cars along the road (100 m radius). The air originated from the sector between the  
310 South and East (5 km) may bring the anthropogenic emission to the site. Ambient air was introduced  
into the instruments by use of a 6 mm outer diameter Teflon tube. The inlet of the Teflon tube was  
outside the building through the window. The data for comparison were averaged to 1min. Fig. 8 (a)  
shows the temporal variations of NO<sub>2</sub> concentrations measured by the CEAS and CRDS instruments.  
The nighttime NO<sub>2</sub> was in the range of 35 ppb to 3 ppb. The NO<sub>2</sub> concentrations and variations  
315 measured by the CRDS instrument were consistent with those measured by the CEAS instrument. The  
least-squares analysis showed that the slope and intercept of the regression line were 1.042  $\pm$  0.002 and  
(-0.393  $\pm$  0.040) ppb, respectively as shown in Fig. 8. However, the results revealed a discrepancy  
where rapid NO<sub>2</sub> variations appeared. We attribute this discrepancy to the slight difference between the  
two inlets of the instruments when large NO<sub>2</sub> was rapidly injected into the atmosphere. In general, the  
320 CRDS instrument has substantive advantages for retrieving rapid variations of NO<sub>2</sub> plums due to its  
high time resolution and high sensitivity.

The comparison of NO concentrations measured by the dual-channel CRDS instrument and CL  
analyzer was conducted under a variety of sampling conditions for a total of seven days at the site  
described previously. Both instruments were attached to the same air sample inlet. The data sets from  
325 the CRDS instrument and CL analyzer were highly correlated over wide concentration ranges of NO.  
Fig. 9 (b) shows the relationship between NO concentrations observed by the CRDS and CL methods.  
The slope and intercept of the regression line were 0.959  $\pm$  0.007 and 0.352  $\pm$  0.013 ppb. The  
correlation coefficient is R<sup>2</sup>=0.99. The CL analyzer is capable of measuring NO reliably. Therefore, the  
dual-channel CRDS instrument is also considered to be a reliable method for the measurement NO.

#### 330 4.3 On-road measurements of vehicle NO<sub>2</sub>/NO<sub>x</sub> emission.

In order to retrieval the vehicle emissions on road, field measurements were performed in Hefei





from 15:00 to 16:00 CST on 17 December 2018. The CRDS instrument was powered by a lithium battery, and ambient air was pumped into the system through an inlet fixed on the roof of the car. The vehicle speed is about 50 km/h. In order to get the discrepancy of vehicle emissions in urban and suburban areas, the car travels along these areas. Fig. 10 shows a picture of the movable van loaded with CRDS instrument and the position of the sampling inlet, about 1.5 m above ground. illustrates the route in Hefei and the drive track is colored logarithmically with respect to measured NO<sub>x</sub>, NO<sub>2</sub> and NO. The NO<sub>2</sub> concentration ranged from 1.5 ppb to 133.3 ppb and NO ranged from detection limit to 554.7 ppb respectively. The mean concentrations of NO and NO<sub>2</sub> were 140 ppb and 54.9 ppb, respectively. NO and NO<sub>2</sub> concentration were higher in urban area than in suburban area. Large plumes of NO were found at the crossroads with heavy traffic or converged with heavy-duty diesel vehicles. [NO<sub>2</sub>] / [NO<sub>x</sub>] ratio was about 19%, a number that is larger than the results in USA (Wild et al., 2017). Because the NO<sub>2</sub> to NO<sub>x</sub> emissions ratio affects ozone production and spatial distribution, more efforts should be done to provide a constraint on emissions inventories used in air quality modeling. The mobile CRDS instrument provides a good method to retrieve the direct vehicle NO<sub>x</sub> emission and plume NO<sub>2</sub> to NO<sub>x</sub> ratio due to its easy deployment and high temporal resolution.

## 5. Conclusion

Demonstration of a compact, sensitive, and accurate instrument for detection trace amounts of NO<sub>2</sub> and NO<sub>x</sub> in ambient air has been achieved by using diode-laser cavity ring-down spectroscopy with the center wavelength of 403.64 nm. Minimum detection limits of NO<sub>2</sub> and NO<sub>x</sub> were estimated to be 0.030 ppb and 0.040 ppb at an integration time of 1 s when zero air is sampled with measurement accuracy of ±5%. Measurements of NO<sub>2</sub> using dual-channel CRDS instrument and CL analyzer on standard mixtures were performed in the present work which demonstrated a good correlation between these techniques. In order to confirm the reliability of the dual-channel CRDS instrument in the field atmosphere. Continuous measurement was conducted and the stability of the instrument was shown. When comparing the dual-channel CRDS instrument for NO<sub>2</sub> measurement with a CEAS instrument and NO measurement with the CL analyzer in the field, the results both showed a good correlation.

The CRDS instrument was deployed in a movable car to monitor NO and NO<sub>2</sub> emission on road. The advantage of high time resolution of the instrument can provide a direct method for on-road vehicle plumes measurement. Meanwhile, the instrument has high detection sensitivity, which can also provide a new detection technique for chemistry model verification. The instruments developed could lead to the wider application for ambient air quality monitoring and will be useful to investigate photochemistry in the atmosphere more precisely.

## Acknowledgments

This work was supported by National Natural Science Foundation of China (61575206, 91644107, 41571130023 and 61805257) and the National Key Research and Development Program of China (2017YFC0209401, 2017YFC0209403).

## References

Ayres, B. R., Allen, H. M., Draper, D. C., Brown, S. S., Wild, R. J., Jimenez, J. L., Day, D. A., Campuzano-Jost, P., Hu, W., de Gouw, J., Koss, A., Cohen, R. C., Duffey, K. C., Romer, P., Baumann, K., Edgerton, E., Takahama, S., Thornton, J. A., Lee, B. H., Lopez-Hilfiker, F. D., Mohr, C., Wennberg, P. O., Nguyen, T. B., Teng, A., Goldstein, A. H., Olson, K., and Fry, J. L.: Organic



- nitrate aerosol formation via  $\text{NO}_3$  + biogenic volatile organic compounds in the southeastern United States, *Atmos. Chem. Phys.*, 15, 13377-13392, doi: 10.5194/acp-15-13377-2015, 2015.
- 375 Brent, L. C., Thorn, W. J., Gupta, M., Leen, B., Stehr, J. W., He, H., Arkinson, H. L., Weinheimer, A., Garland, C., Pusede, S. E., Wooldridge, P. J., Cohen, R. C., and Dickerson, R. R.: Evaluation of the use of a commercially available cavity ringdown absorption spectrometer for measuring  $\text{NO}_2$  in flight, and observations over the Mid-Atlantic States, during DISCOVER-AQ, *J. Atmos. Chem.*, 72, 503-521, doi: 10.1007/s10874-013-9265-6, 2013.
- 380 Brown, S. S., Dibb, J. E., Stark, H., Aldener, M., Vozella, M., Whitlow, S., Williams, E. J., Lerner, B. M., Jakoubek, R., Middlebrook, A. M., DeGouw, J. A., Warneke, C., Goldan, P. D., Kuster, W. C., Angevine, W. M., Sueper, D. T., Quinn, P. K., Bates, T. S., Meagher, J. F., Fehsenfeld, F. C., and Ravishankara, A. R.: Nighttime removal of  $\text{NO}_x$  in the summer marine boundary layer, *Geophys. Res. Lett.*, 31, 1-5, doi: 10.1029/2004gl019412, 2004.
- 385 Burgard, D. A., Bishop, G. A., Stadtmuller, R. S., Dalton, T. R., and Stedman, D. H.: Spectroscopy applied to on-road mobile source emissions, *Appl. Spectrosc.*, 60, 135a-148a, doi: 10.1366/000370206777412185, 2006a.
- Burgard, D. A., Bishop, G. A., Stedman, D. H., Gessner, V. H., and Daeschlein, C.: Remote sensing of in-use heavy-duty diesel trucks, *Environ. Sci. Technol.*, 40, 6938-6942, doi: 10.1021/es060989a, 2006b.
- 390 Carslaw, D. C., and Beevers, S. D.: Investigating the potential importance of primary  $\text{NO}_2$  emissions in a street canyon, *Atmos. Environ.*, 38, 3585-3594, doi: 10.1016/j.atmosenv.2004.03.041, 2004.
- Carslaw, D. C.: Evidence of an increasing  $\text{NO}_2/\text{NO}_x$  emissions ratio from road traffic emissions, *Atmos. Environ.*, 39, 4793-4802, doi: 10.1016/j.atmosenv.2005.06.023, 2005.
- 395 Castellanos, P., Luke, W. T., Kelley, P., Stehr, J. W., Ehrman, S. H., and Dickerson, R. R.: Modification of a commercial cavity ring-down spectroscopy  $\text{NO}_2$  detector for enhanced sensitivity, *Rev. Sci. Instrum.*, 80, doi: 10.1063/1.3244090, 2009.
- Chen, Y., Yang, C. Q., Zhao, W. X., Fang, B., Xu, X. Z., Gai, Y. B., Lin, X. X., Chen, W. D., and Zhang, W. J.: Ultra-sensitive measurement of peroxy radicals by chemical amplification broadband cavity-enhanced spectroscopy, *Analyst*, 141, 5870-5878, doi: 10.1039/c6an01038e, 2016.
- 400 Crutzen, P. J.: Role of  $\text{NO}$  and  $\text{NO}_2$  in the chemistry of the troposphere, *Annu. Rev. Earth Planet. Sci.*, 7, 443-472, doi: 10.1146/annurev.ea.07.050179.002303, 1979.
- Day, D. A., Wooldridge, P. J., Dillon, M. B., Thornton, J. A., and Cohen, R. C.: A thermal dissociation laser-induced fluorescence instrument for in situ detection of  $\text{NO}_2$ , peroxy nitrates, alkyl nitrates, and  $\text{HNO}_3$ , *J. Geophys. Res. Atmos.*, 107, ACH 4-1-ACH 4-14, doi: 10.1029/2001jd000779, 2002.
- 405 Duan J., Qin M., Ouyang, B., Fang, W., Li, X., Lu, K. D., Tang, K., Liang, S. X., Meng, F. H., Hu, Z. K., Xie, P.H., Liu, W. Q., Rolf Häslér, Development of an incoherent broadband cavity-enhanced absorption spectrometer for in situ measurements of HONO and  $\text{NO}_2$ . *Atmos. Meas. Tech.*, 11, 4531-4543, doi: 10.5194/amt-11-4531-2018, 2018.
- 410 Dunlea, E. J., Herndon, S. C., Nelson, D. D., Volkamer, R. M., San Martini, F., Sheehy, P. M., Zahniser, M. S., Shorter, J. H., Wormhoudt, J. C., Lamb, B. K., Allwine, E. J., Gaffney, J. S., Marley, N. A., Grutter, M., Marquez, C., Blanco, S., Cardenas, B., Retama, A., Villegas, C. R. R., Kolb, C. E., Molina, L. T., and Molina, M. J.: Evaluation of nitrogen dioxide chemiluminescence monitors in a polluted urban environment, *Atmos. Chem. Phys.*, 7, 2691-2704, doi: 10.5194/acp-7-2691-2007, 2007.
- 415 Fahey, D. W., Eubank, C. S., Hubler, G., and Fehsenfeld, F. C.: Evaluation of a Catalytic Reduction



- Technique for the Measurement of Total Reactive Odd-Nitrogen  $\text{NO}_y$  in the Atmosphere, *J. Atmo. Chem.*, 3, 435-468, doi: 10.1007/bf00053871, 1985.
- 420 Fuchs, H., Dube, W. P., Lerner, B. M., Wagner, N. L., Williams, E. J., and Brown, S. S.: A Sensitive and Versatile Detector for Atmospheric  $\text{NO}_2$  and  $\text{NO}_x$  Based on Blue Diode Laser Cavity Ring-Down Spectroscopy, *Environ. Sci. Technol.*, 43, 7831-7836, doi: 10.1021/es902067h, 2009.
- 425 Fuchs, H., Ball, S. M., Bohn, B., Brauers, T., Cohen, R. C., Dorn, H. P., Dube, W. P., Fry, J. L., Haseler, R., Heitmann, U., Jones, R. L., Kleffmann, J., Mentel, T. F., Musgen, P., Rohrer, F., Rollins, A. W., Ruth, A. A., Kiendler-Scharr, A., Schlosser, E., Shillings, A. J. L., Tillmann, R., Varma, R. M., Venables, D. S., Tapia, G. V., Wahner, A., Wegener, R., Wooldridge, P. J., and Brown, S. S.: Intercomparison of measurements of  $\text{NO}_2$  concentrations in the atmosphere simulation chamber SAPHIR during the  $\text{NO}_3\text{Comp}$  campaign, *Atmo.Meas.Tech.*, 3, 21-37, doi: 10.5194/amt-3-21-2010, 2010.
- 430 Gherman, T., Venables, D. S., Vaughan, S., Orphal, J., and Ruth, A. A.: Incoherent broadband cavity-enhanced absorption spectroscopy in the near-ultraviolet: Application to HONO and  $\text{NO}_2$ , *Environ. Sci. Technol.*, 42, 890-895, doi: 10.1021/es0716913, 2008.
- Herndon, S. C., Shorter, J. H., Zahniser, M. S., Nelson, D. D., Jayne, J., Brown, R. C., Miake-Lye, R. C., Waitz, I., Silva, P., Lanni, T., Demerjian, K., and Kolb, C. E.:  $\text{NO}$  and  $\text{NO}_2$  emission ratios measured from in-use commercial aircraft during taxi and takeoff, *Environ. Sci. Technol.*, 38, 6078-6084, doi: 10.1021/es049701c, 2004.
- 435 Herndon, S. C., Shorter, J. H., Zahniser, M. S., Wormhoudt, J., Nelson, D. D., Demerjian, K. L., and Kolb, C. E.: Real-time measurements of  $\text{SO}_2$ ,  $\text{H}_2\text{CO}$ , and  $\text{CH}_4$  emissions from in-use curbside passenger buses in New York City using a chase vehicle, *Environ. Sci. Technol.*, 39, 7984-7990, doi: 10.1021/es0482942, 2005.
- 440 Hueglin, C., Buchmann, B., and Weber, R. O.: Long-term observation of real-world road traffic emission factors on a motorway in Switzerland, *Atmos. Environ.*, 40, 3696-3709, doi: 10.1016/j.atmosenv.2006.03.020, 2006.
- Hu, R. Z., Wang, D., Xie, P. H., Chen, H., Ling, L., "Diode Laser Cavity Ring-Down Spectroscopy for Atmospheric  $\text{NO}_2$  Measurement," *Acta. Optica. Sinica.* 36, 0230006, 2016.
- 445 Jagerska, J., Jouy, P., Tuzson, B., Looser, H., Mangold, M., Soltic, P., Hugi, A., Bronnimann, R., Faist, J., and Emmenegger, L.: Simultaneous measurement of  $\text{NO}$  and  $\text{NO}_2$  by dual-wavelength quantum cascade laser spectroscopy, *Opt. Express*, 23, 1512-1522, doi: 10.1364/oe.23.001512, 2015.
- Jaramillo, P., and Muller, N. Z.: Air pollution emissions and damages from energy production in the US: 2002-2011, *Energy Policy*, 90, 202-211, doi: 10.1016/j.enpol.2015.12.035, 2016.
- 450 Karpf, A., Qiao, Y. H., and Rao, G. N.: Ultrasensitive, real-time trace gas detection using a high-power, multimode diode laser and cavity ringdown spectroscopy, *Appl. Optics*, 55, 4497-4504, doi: 10.1364/ao.55.004497, 2016.
- Kasyutich, V. L., Martin, P. A., and Holdsworth, R. J.: Phase-shift off-axis cavity-enhanced absorption detector of nitrogen dioxide, *Meas. Sci. Technol.*, 17, 923-931, doi: 10.1088/0957-0233/17/4/044, 2006.
- 455 Kebedian, P. L., Wood, E. C., Herndon, S. C., and Freedman, A.: A practical alternative to chemiluminescence-based detection of nitrogen dioxide: Cavity attenuated phase shift spectroscopy, *Environ.Sci.Technol.*, 42, 6040-6045, doi: 10.1021/es703204j, 2008.
- Lal, D. R., Clark, I., Shalkow, J., Downey, R. J., Shorter, N. A., Klimstra, D. S., and La Quaglia, M. P.: 460 Primary epithelial lung malignancies in the pediatric population, *Pediatr. Blood Cancer*, 45, 683-686,



- doi: 10.1002/pbc.20279, 2005.
- Li, Y. Q., Demerjian, K. L., Zahniser, M. S., Nelson, D. D., McManus, J. B., and Herndon, S. C.: Measurement of formaldehyde, nitrogen dioxide, and sulfur dioxide at Whiteface Mountain using a dual tunable diode laser system, *J. Geophys. Res. Atmos.*, 109, 11, doi: 10.1029/2003jd004091, 2004.
- 465 Li, Z. Y., Hu, R. Z., Xie, P. H., Wang, H.C., Lu, K. D., Wang, D.: Intercomparison of in situ CRDS and CEAS for measurements of atmospheric N<sub>2</sub>O<sub>5</sub> in Beijing, China. *Science of the Total Environment*, 613 – 614, 131 – 139. doi: 10.1016/j.scitotenv.2017.08.302, 2018.
- Li, Z. Y., Hu, R. Z., Xie, P. H., Chen, H., Wu S. Y., Wang, F. Y., Wang, Y. H., Ling, L. Y., Liu, J. G., and  
470 Liu, W. Q.: Development of a portable cavity ring down spectroscopy instrument for simultaneous, in situ measurement of NO<sub>3</sub> and N<sub>2</sub>O<sub>5</sub>. *Optics Express*. 26, A433-A449. <https://doi.org/10.1364/OE.26.00A433.P>, 2018.
- Matsumi, Y., Taketani, F., Takahashi, K., Nakayama, T., Kawai, M., and Miyao, Y.: Fluorescence detection of atmospheric nitrogen dioxide using a blue light-emitting diode as an excitation source, *Appl. Optics*, 49, 3762-3767, doi: 10.1364/ao.49.003762, 2010.
- 475 Matsumoto, J., Hirokawa, J., Akimoto, H., and Kajii, Y.: Direct measurement of NO<sub>2</sub> in the marine atmosphere by laser-induced fluorescence technique, *Atmos. Environ.*, 35, 2803-2814, doi: 10.1016/s1352-2310(01)00078-4, 2001.
- Novikov, S., Lebedeva, N., Satrapinski, A., Walden, J., Davydov, V., and Lebedev, A.: Graphene based  
480 sensor for environmental monitoring of NO<sub>2</sub>, *Sens. Actuator B-Chem.*, 236, 1054-1060, doi: 10.1016/j.snb.2016.05.114, 2016.
- Osthoff, H. D., Brown, S. S., Ryerson, T. B., Fortin, T. J., Lerner, B. M., Williams, E. J., Pettersson, A., Baynard, T., Dube, W. P., Ciciora, S. J., and Ravishankara, A. R.: Measurement of atmospheric NO<sub>2</sub> by pulsed cavity ring-down spectroscopy, *J. Geophys. Res.-Atmos.*, 111, doi:  
485 10.1029/2005jd006942, 2006.
- Osthoff, H. D., Pilling, M. J., Ravishankara, A. R., and Brown, S. S.: Temperature dependence of the NO<sub>3</sub> absorption cross-section above 298 K and determination of the equilibrium constant for NO<sub>3</sub>+NO<sub>2</sub><-> N<sub>2</sub>O<sub>5</sub> at atmospherically relevant conditions, *Phys. Chem. Chem.Phys.*, 9, 5785-5793, doi: 10.1039/b709193a, 2007.
- 490 Paul, D., Furgeson, A., and Osthoff, H. D.: Measurements of total peroxy and alkyl nitrate abundances in laboratory-generated gas samples by thermal dissociation cavity ring-down spectroscopy, *Rev. Sci. Instrum.*, 80, doi: 10.1063/1.3258204, 2009.
- Platt, U. F., Winer, A. M., Biermann, H. W., Atkinson, R., and Pitts, J. N.: Measurement of nitrate radical concentrations in continental air, *Environ. Sci. Tech.*, 18, 365-369, doi:  
495 10.1021/es00123a015, 1984.
- R. McLaren, P. W., D. Majonis, J. McCourt, J. D. Halla, and J. Brook: NO<sub>3</sub> radical measurements in a polluted marine environment: links to ozone formation, *Atmo.Chem.Phys.*, 10, 4187–4206, doi: 10.5194/acp-10-4187-2010, 2010.
- Ridley, B. A., and Howlett, L. C.: An instrument for nitric oxide measurements in the stratosphere, *Rev. Sci. Instrum.*, 45, 742-746, doi: 10.1063/1.1686726, 1974.
- 500 Sadanaga, Y., Yuba, A., Kawakami, J., Takenaka, N., Yamamoto, M., and Bandow, H.: A gaseous nitric acid analyzer for the remote atmosphere based on the scrubber difference/NO-ozone chemiluminescence method, *Anal. Sci.*, 24, 967-971, doi: 10.2116/analsci.24.967, 2008.
- Sadanaga, Y., Suzuki, K., Yoshimoto, T., and Bandow, H.: Direct measurement system of nitrogen



- 505 dioxide in the atmosphere using a blue light-emitting diode induced fluorescence technique, *Rev. Sci. Instrum.*, 85, 5, doi: 10.1063/1.4879821, 2014.
- Sander, S. P., Friedl, R. R., Golden, D. M., Kurylo, M. J., Huie, R. E., O., V. L., Moortgat, G. K., Ravishankara, A. R., and Kolb, C. E., Molina, M. J., and Finlayson-Pitts, B. J.: Chemical Kinetics and Photochemical Data for Use in Atmospheric Studies Evaluation Number 15 Jet Propulsion Laboratory, National Aeronautics and Space Administration/Jet Propulsion Laboratory/ California Institute of Technology, Pasadena, CA, 2006.
- 510 Shi, Y. L., Cui, S. h., and Xu, S.: Factor decomposition of nitrogen oxide emission of China industrial energy consumption, *Environ. Sci. Tech.*, 37, 355-362., 2014.
- Sobanski, N., Tang, M. J., Thieser, J., Schuster, G., Pohler, D., Fischer, H., Song, W., Sauvage, C., Williams, J., Fachinger, J., Berkes, F., Hoor, P., Platt, U., Lelieveld, J., and Crowley, J. N.: Chemical and meteorological influences on the lifetime of NO<sub>3</sub> at a semi-rural mountain site during PARADE, *Atmos. Chem. Phys.*, 16, 4867-4883, doi: 10.5194/acp-16-4867-2016, 2016.
- Taketani, F., Kawai, M., Takahashi, K., and Matsumi, Y.: Trace detection of atmospheric NO<sub>2</sub> by laser-induced fluorescence using a GaN diode laser and a diode-pumped YAG laser, *Appl. Optics*, 46, 907-915, doi: 10.1364/ao.46.000907, 2007.
- 520 Thieser, J., Schuster, G., Schuladen, J., Phillips, G. J., Reiffs, A., Parchatka, U., Pohler, D., Lelieveld, J., and Crowley, J. N.: A two-channel thermal dissociation cavity ring-down spectrometer for the detection of ambient NO<sub>2</sub>, RO<sub>2</sub>NO<sub>2</sub> and RONO<sub>2</sub>, *Atmos. Meas. Tech.*, 9, 553-576, doi: 10.5194/amt-9-553-2016, 2016.
- 525 Villena, G., Bejan, I., Kurtenbach, R., Wiesen, P., and Kleffmann, J.: Development of a new Long Path Absorption Photometer (LOPAP) instrument for the sensitive detection of NO<sub>2</sub> in the atmosphere, *Atmos. Meas. Tech.*, 4, 1663-1676, doi: 10.5194/amt-4-1663-2011, 2011.
- Villena, G., Bejan, I., Kurtenbach, R., Wiesen, P., and Kleffmann, J.: Interferences of commercial NO<sub>2</sub> instruments in the urban atmosphere and in a smog chamber, *Atmos. Meas. Tech.*, 5, 149-159, doi: 10.5194/amt-5-149-2012, 2012.
- 530 Vogt, R., Scheer, V., Casati, R., and Benter, T.: On-road measurement of particle emission in the exhaust plume of a diesel passenger car, *Environ. Sci. Tech.*, 37, 4070-4076, doi: 10.1021/es0300315, 2003.
- Voigt, S., Orphal, J., and Burrows, J. P.: The temperature and pressure dependence of the absorption cross-sections of NO<sub>2</sub> in the 250-800 nm region measured by Fourier-transform spectroscopy, *J. Photochem. Photobiol., A-Chemistry*, 149, 1-7, doi: 10.1016/s1010-6030(01)00650-5, 2002.
- 535 Wada, R., and Orr-Ewing, A. J.: Continuous wave cavity ring-down spectroscopy measurement of NO<sub>2</sub> mixing ratios in ambient air, *Analyst*, 130, 1595-1600, doi: 10.1039/b511115c, 2005.
- Wagner, N. L., Dube, W. P., Washenfelder, R. A., Young, C. J., Pollack, I. B., Ryerson, T. B., and Brown, S. S.: Diode laser-based cavity ring-down instrument for NO<sub>3</sub>, N<sub>2</sub>O<sub>5</sub>, NO, NO<sub>2</sub> and O<sub>3</sub> from aircraft, *Atmos. Meas. Tech.*, 4, 1227-1240, doi: 10.5194/amt-4-1227-2011, 2011.
- 540 Wagner, N. L., Riedel, T. P., Young, C. J., Bahreini, R., Brock, C. A., Dube, W. P., Kim, S., Middlebrook, A. M., Ozturk, F., Roberts, J. M., Russo, R., Sive, B., Swarthout, R., Thornton, J. A., VandenBoer, T. C., Zhou, Y., and Brown, S. S.: N<sub>2</sub>O<sub>5</sub> uptake coefficients and nocturnal NO<sub>2</sub> removal rates determined from ambient wintertime measurements, *J. Geophys. Res.-Atmos.*, 118, 9331-9350, doi: 10.1002/jgrd.50653, 2013.
- 545 Wang, D., Hu, R. Z., Xie, P. H., Liu, J. G., Liu, W. Q., Qin, M., Ling, L.Y., Zeng, Y., Chen, H., Xing, X.B., Zhu, G. L., Wu, J., Duan, J., Lu, X., Shen, L.L., 2015. Diode laser cavity ring-down

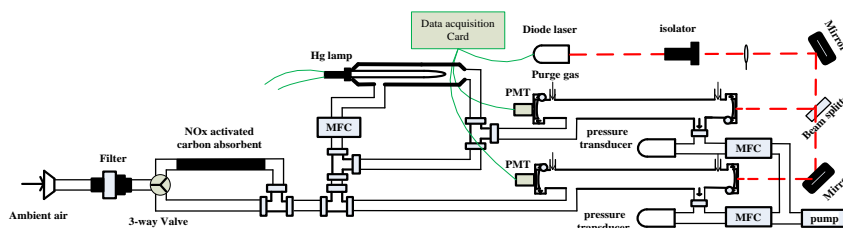


- spectroscopy for in situ measurement of NO<sub>3</sub> radical in ambient air. *J. Quant.Spectrosc. Radiat. Transf.* 166, 23–29, doi: 10.1016/j.jqsrt.2015.07.005, 2015.
- 550 Wang, T., Cheung, V. T. F., Anson, M., and Li, Y. S.: Ozone and related gaseous pollutants in the boundary layer of eastern China: Overview of the recent measurements at a rural site, *Geophys. Res. Lett.*, 28, 2373-2376, doi: 10.1029/2000gl012378, 2001.
- Westerdahl, D.: Avoiding Measurement Errors When Monitoring Fine and Ultrafine PM for Exposure and Epidemiology Studies, *Epidemiology*, 19, S360-S360, 2008.
- 555 Wild, R. J., Edwards, P. M., Dube, W. P., Baumann, K., Edgerton, E. S., Quinn, P. K., Roberts, J. M., Rollins, A. W., Veres, P. R., Warneke, C., Williams, E. J., Yuan, B., and Brown, S. S.: A measurement of total reactive nitrogen, NO<sub>y</sub>, together with NO<sub>2</sub>, NO, and O<sub>3</sub> via cavity ring-down spectroscopy, *Environ. Sci. Technol.*, 48, 9609-9615, doi: 10.1021/es501896w, 2014.
- 560 Wild, R. J., Dube, W. P., Aikin, K. C., Eilerman, S. J., Neuman, J. A., Peischl, J., Ryerson, T. B., and Brown, S. S.: On-road measurements of vehicle NO<sub>2</sub>/NO<sub>x</sub> emission ratios in Denver, Colorado, USA, *Atmos. Environ.*, 148, 182-189, doi: 10.1016/j.atmosenv.2016.10.039, 2017.
- Wu, T., Zhao, W., Chen, W., Zhang, W., and Gao, X.: Incoherent broadband cavity enhanced absorption spectroscopy for in situ measurements of NO<sub>2</sub> with a blue light emitting diode, *Appl. Phys. B-Lasers and Optics*, 94, 85-94, doi: 10.1007/s00340-008-3308-8, 2009.
- 565 Xu, Z., Wang, T., Xue, L. K., Louie, P. K. K., Luk, C. W. Y., Gao, J., Wang, S. L., Chai, F. H., and Wang, W. X.: Evaluating the uncertainties of thermal catalytic conversion in measuring atmospheric nitrogen dioxide at four differently polluted sites in China, *Atmos. Environ.*, 76, 221-226, doi: 10.1016/j.atmosenv.2012.09.043, 2013.
- 570 Yamamoto, Y., Sumizawa, H., Yamada, H., and Tonokura, K.: Real-time measurement of nitrogen dioxide in vehicle exhaust gas by mid-infrared cavity ring-down spectroscopy, *Appl. Phys. B*, 105, 923-931, doi: 10.1007/s00340-011-4647-4, 2011.
- Yang, W., and Omaye, S. T.: Air pollutants, oxidative stress and human health, *Mutat. Res. Genet. Toxicol. Environ. Mutagen.*, 674, 45-54, doi: 10.1016/j.mrgentox.2008.10.005, 2009.
- 575 Yuba, A., Sadanaga, Y., Takami, A., Hatakeyama, S., Takenaka, N., and Bandow, H.: Measurement System for Particulate Nitrate Based on the Scrubber Difference NO-O<sub>3</sub> Chemiluminescence Method in Remote Areas, *Anal. chem.*, 82, 8916-8921, doi: 10.1021/ac101704w, 2010.

Table 1 Comparison of NO<sub>2</sub> detection limits based on optical methods.

Principle of measurement	Laser power	Wavelength range/nm	Detection limit	Reference
Cw-CRDS	5mW(1MHz)	410	80ppt/50s	(Wada and Orr-Ewing, 2005)
ND:YAG laser CRDS	1mJ	532	40ppt/1s	(Osthoff et al., 2006)
pDL-CRDS	40 mW (2KHZ-10%)	404	22ppt/1s(2σ)	(Fuchs et al., 2009)
Fabry-Perot (FP) pDL-CRDS	1.1w (4KHZ-10%)	400	38ppt/128ms	(Karpf et al., 2016)
commercial DL-CRDS	1.2KHZ	407.38	60ppt/60s(3σ)	(Castellanos et al., 2009)
LED-based commercial CRD	355 mW	397-412(405)	80ppt/60s	(Brent et al., 2013)
LED-CEAS	340mw	455	2.2ppb/100s(1σ)	(Wu et al., 2009)
Xe lamp DOAS		295–492 nm	2ppb/8-12min	(R. McLaren, 2010)
CAPS		440	60ppt/10s(3σ)	(Kebabian et al., 2008)
diode-pumped Nd:YAG laser-LIF	15mw(14KHz)	473	140/60s	(Taketani et al., 2007)
blue LED-IF	17.7mw(10KHz)	435	9.8ppb/60	(Matsumi et al., 2010)
pulsed blue light LED-LIF	22mw	430	7ppb/1min	(Sadanaga et al., 2014)
pDL-CRDS	60mw	403.64	30ppt/1s	This work

580 CRDS=cavity ring-down spectroscopy; CEAS=cavity-enhanced absorption spectroscopy; BB=broadband; DOAS=differential optical absorption spectroscopy; cw=continuous-wave diode laser. LIF=laser induced fluorescence; CAPS= cavity attenuated phase shift spectroscopy; pDL=pulsed diode laser.



585

Fig. 1. Schematic of dual-channel Cavity Ring down Spectroscopy system.

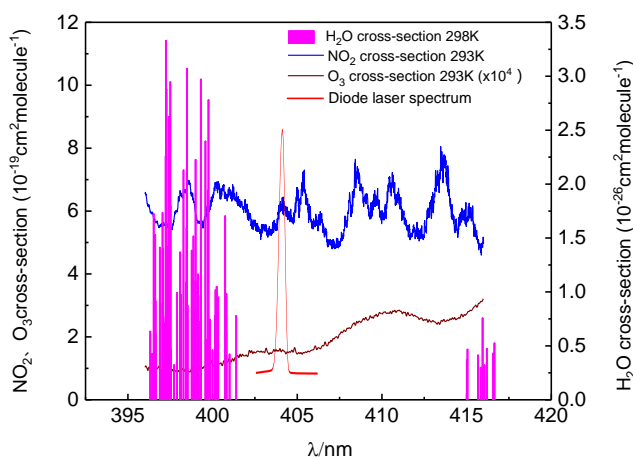
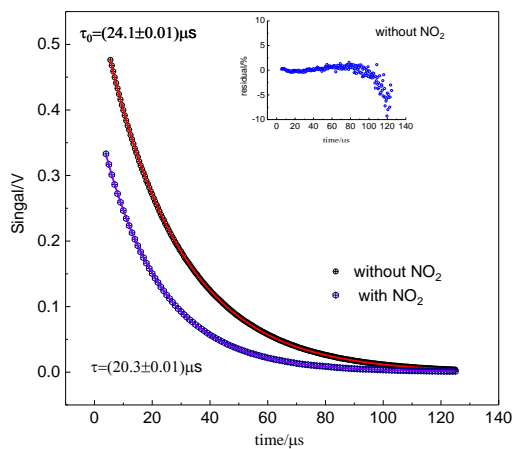


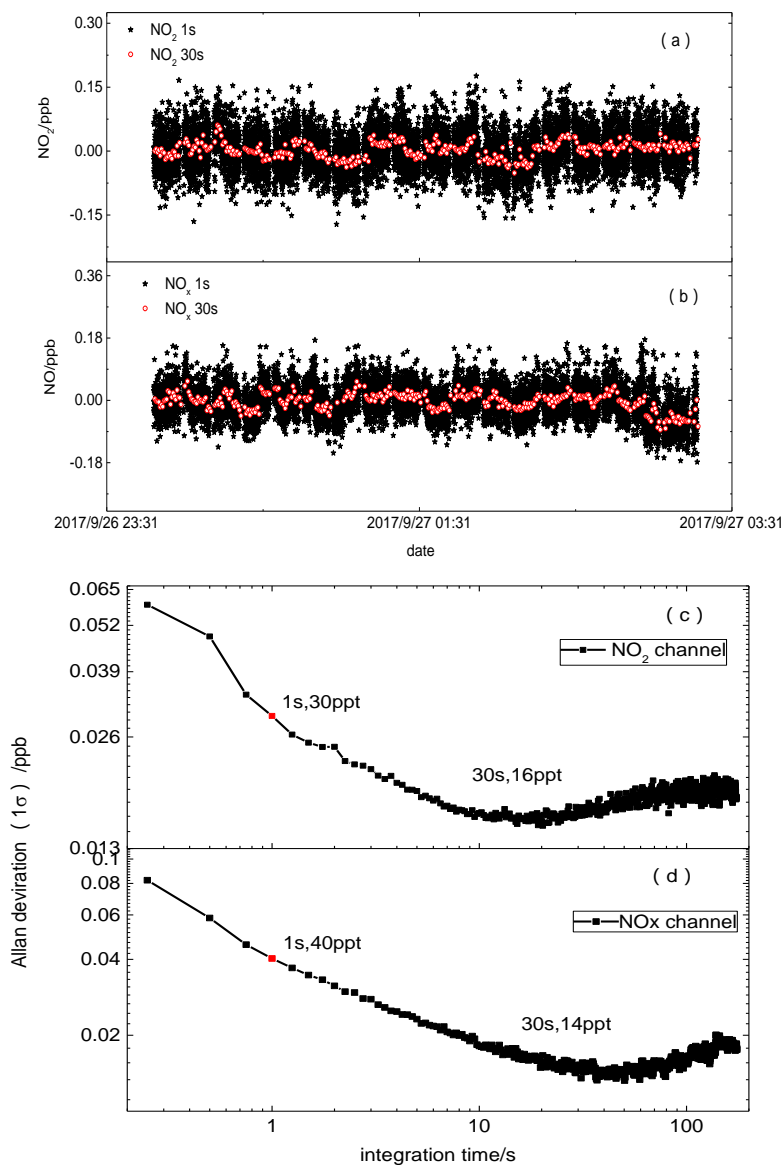
Fig. 2. Cross section of the  $\text{NO}_3$  radical,  $\text{NO}_2$ ,  $\text{O}_3$ , water vapor, and diode laser spectrum.



590

Fig. 3. Different cavity ring-down signals and fitting results in the absence and presence of  $\text{NO}_2$ . The small figure in the upper right corner is the fitting residual.





595

Fig. 4. (a)(b) Continuous time series measurement when the instrument sampled only zero air, averaged to 1s for  $\text{NO}_2$  and  $\text{NO}_x$  channels (black dots), the red dots show the data averaged to 30s; (c)(d): Allan deviation plots for  $\text{NO}_2$  concentration in two channels. The minimum value equals the optimum integration time.

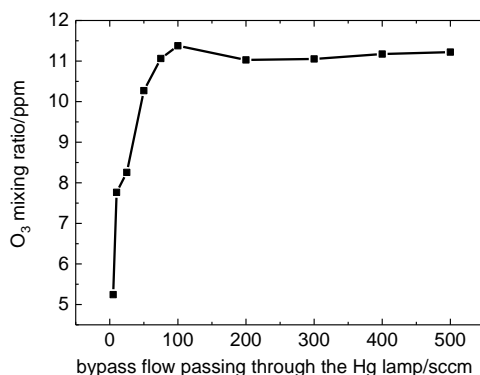


Fig. 5. O<sub>3</sub> mixing ratio when changing the bypass flow passing through Hg lamp.

600

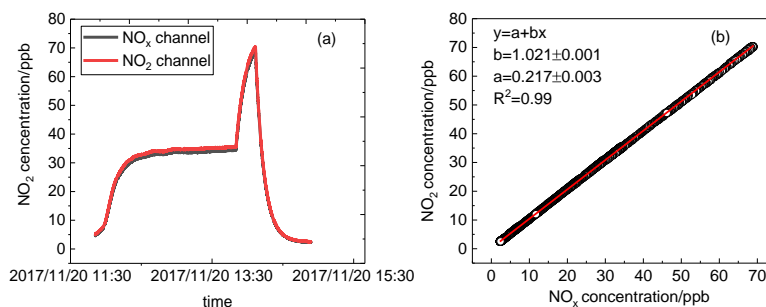


Fig. 6. (a) Time series of NO<sub>2</sub> concentration sampled standard mixtures by CRDS instrument in two channels with mercury pen-ray lamp switched on. (b) A correlation plot between the data from two channels.

605

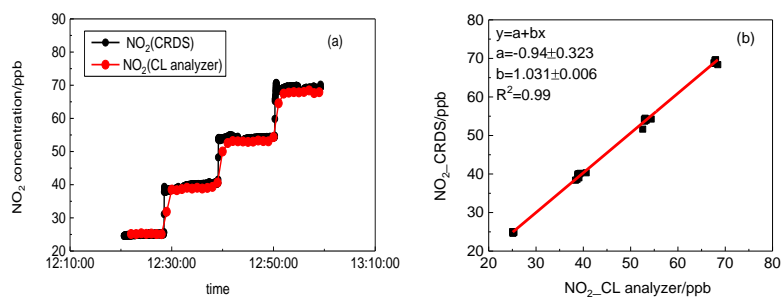


Fig. 7. (a) Time series of NO<sub>2</sub> concentration sampled standard mixtures by CRDS instrument and CL analyzer. The time resolution for CRDS instrument and CL analyzer are 1s and 1min, respectively. (b) A correlation plot between the data from the CRDS instrument and the CL analyzer (data averaged to 1min). The fitting result gave a gradient of 1.031 and an intercept of -0.940 ppb, with linear correlation factor of 0.99.

610

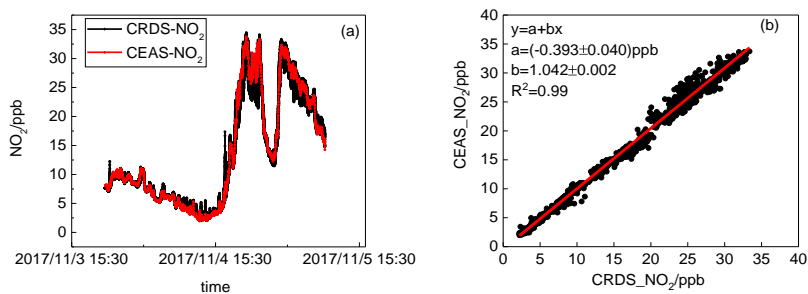


Fig. 8. (a)  $\text{NO}_2$  mixing ratios by CEAS (1 min average) and CRDS (1 s average) instruments, (b) Scatter plots for the  $\text{NO}_2$  dataset from CRDS and CEAS instrument. The red lines illustrate the linear regression (Data averaged to 1 min base).

615

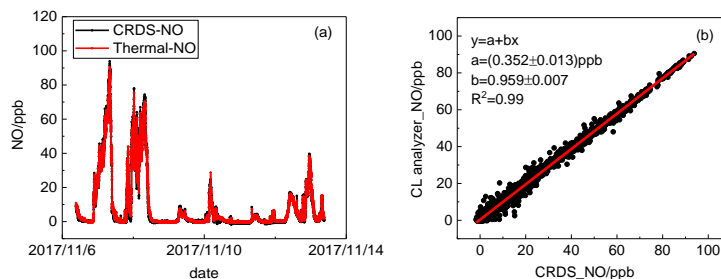


Fig. 9. (a) Time series of NO by dual-CRDS instrument and CL analyzer. (b) A correlation between two instruments is shown and data for correlation analysis is averaged in 1 min.

620

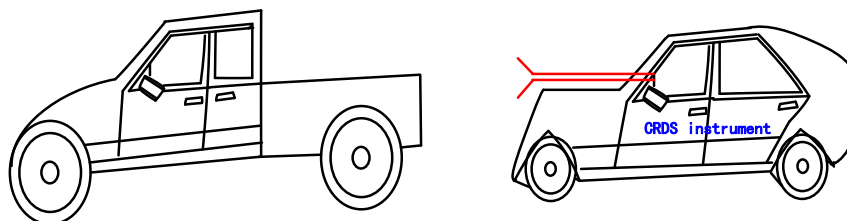


Fig. 10 The diagram of the movable van loaded with CRDS instrument.



625

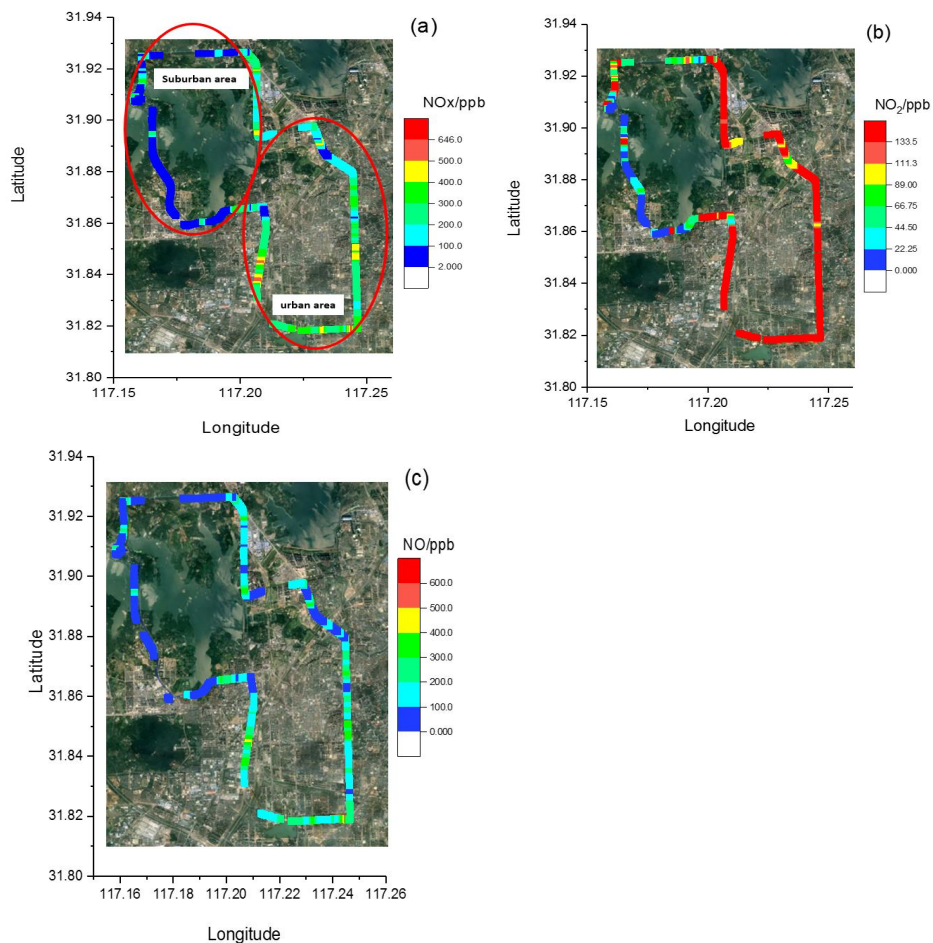


Fig. 11. Results of the NO<sub>x</sub> (a), NO<sub>2</sub> (b), NO (c) concentrations around Hefei, China (Data is averaged to 5s).